

LAND CONTAMINATION CORRECTION FOR AMSR2

Suleiman Alswais^{1,2}, Zorana Jelenak^{1,3}, Joseph Sapp^{1,2}, and Paul Chang¹

NOAA/NESDIS/STAR¹, Global Science & Technology, Inc. (GST)², University Corporation for Atmospheric Research (UCAR)³

ABSTRACT

Microwave radiometers are designed to capture the Earth's electromagnetic radiation in the form of brightness temperatures. At low and medium frequencies, the relatively large footprint of microwave radiometers results in mixing land and water brightness temperatures in coastal areas and lakes. This mixing of signals, also known as land contamination, limits the usability of radiometer measurements and makes them unsuitable for geophysical retrievals up to ~ 100 km away from the coastline. In this paper, we present preliminary results of applying a land contamination correction on AMSR2 measurements to extract coastal information. The correction technique relies on calculating the land fraction within AMSR2 footprints using a high-resolution land mask and a representative antenna pattern.

Index Terms— AMSR2, brightness temperatures, land fraction, land contamination, coastal retrievals

1. INTRODUCTION

Over the last few decades, spaceborne measurements have been widely used to monitor the Earth's environment and infer critical geophysical parameters with near global coverage [1-3]. The inferred geophysical parameters include total precipitable water (TPW), cloud liquid water (CLW), precipitation, sea surface temperature (SST), and sea surface wind speed (SSW).

Scientists have developed numerous ways by which these geophysical parameters can be retrieved from radiometer data (e.g. [4], [5], and [6]). The retrieval algorithms exploit the measured brightness temperatures (Tbs) from different channels (different polarization and frequency) to infer the parameters of interest via an inversion process.

By design, radiometers usually have channels that are known to be more sensitive to certain parameters than to others. While Tbs at frequencies up to 11 GHz are primarily proportional to ocean surface parameters, Tbs at higher frequencies have more contribution from the intervening atmosphere.

The use of different radiometer channels leads to different spatial resolutions for the satellite instantaneous

fields of view (IFOV) which vary inversely with frequency. For instance, at C-band the IFOV size of a low earth orbiting instrument is typically around 60 km × 30 km (along-track × cross-track) and decreases to reach few kilometers at W-band (e.g., 5 km × 3 km at 89 GHz).

The large radiometer IFOVs highlight the issue of land contamination in retrieval algorithms. When the IFOV spans land and water scenes (e.g., coastlines), the measured Tb will be a mix between land and water Tbs. For example, horizontally polarized (H-pol) 6 GHz Tbs are typically around 80 k over rain-free open ocean, but it can exceed 200 k over land. A signal mixing of that order can significantly degrade retrievals around coastal areas and inland bodies of water. The amount of mixing depends on the fraction of land and water within the radiometer IFOV.

In this paper, we will briefly describe the application of a land contamination correction technique to extend the usability of the Advanced Microwave Scanning Radiometer-2 (AMSR2) Tbs to coastal areas. We start with a brief description of the AMSR2 instrument and its oceanic environmental data records (EDRs) in Section II, and then a general description of AMSR2 land contamination correction and some preliminary results in Sections III. Conclusions are presented in Section IV.

2. AMSR2

AMSR2 on board the Global Change Observation Mission-Water (GCOM-W) was launched in May 2012 by the Japanese Aerospace Exploration Agency (JAXA). It is a passive remote sensing instrument that acquires microwave emission from the Earth's surface and atmosphere at 6.9, 7.3, 10.65, 18.7, 23.8, 36.5, and 89.0 GHz. It operates at a nominal earth incidence angle (EIA) of 55° which results in a wide swath of 1450 km.

AMSR2 has a 2.0 m aperture diameter antenna that completes one full rotation every 1.5 seconds. It conically scans the Earth's surface to obtain measurements along a semicircular pattern in front of the spacecraft. Table 1 summarizes the different spatial resolutions for all AMSR2 channels.

A suite of oceanic EDRs is derived from AMSR2 that include TPW, CLW, SST, SSW, and precipitation. The operational EDR processing algorithms utilize calibrated AMSR2 Tbs [7] in a robust multi-stage regression-based

retrieval algorithm. A near real time demonstration of these advanced satellite data products can be obtained from [8].

Table 1: AMSR2 Spatial Resolution by Channel

Freq. (GHz)	6.9	7.3	10.6	18.7	23.8	36.5	89
Polarization	Vertical & horizontal						
Along-track IFOV width (km)	62	58	42	22	26	12	5
Cross-track IFOV width (km)	35	34	24	14	15	7	3

3. AMSR2 LAND CONTAMINATION CORRECTION

In this section, the methodology used to correct for land contamination in AMSR2 measurements is described. Land contamination correction is the process of removing the land signal from the measured Tbs. Figure 1 depicts the effect of land contamination on the AMSR2 6 GHz H-pol channel near the coast of Alaska. The significant increase in Tb values is clear as the location of the measurements gets closer to the coastline (red color in the plot).

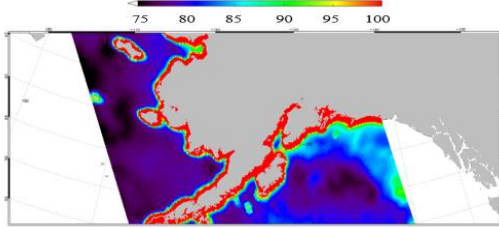


Figure 1: AMSR2 6 GHz H-pol Tb near the coast of Alaska showing land contamination.

The adopted methodology relies on calculating the land fraction (F_{land}) in every Tb measurement. Then, the calculated F_{land} will be used to correct the coastal Tb measurements following Eq. 1 [9]:

$$Tb_{meas} = F_{land} \times Tb_{land} + (1 - F_{land}) \times Tb_{water} \quad (1)$$

Eq. 1 models the measured Tb as a weighted average of land and water signals with F_{land} being the weighting factor. F_{land} is calculated by convolving a land mask with the radiometer antenna pattern. A 1 km binary land mask derived from GMT 5.4.4 [10] and a simulated Gaussian antenna pattern were used to calculate F_{land} for AMSR2. Figure 2 shows the 2-dimensional (2D) Gaussian function used to simulate the AMSR2 antenna for the 6 GHz channel. Panels a and b show the along-track and cross-track antenna patterns, respectively. The x-axis is the distance in km from antenna boresight and the y-axis is the normalized gain. Red curves show the probability density function (PDF), blue curves show the cumulative distribution function (CDF), and green lines show the half-power beam width (HPBW).

Figure 3 shows the calculated F_{land} for the AMSR2 6 GHz channel resulting from the convolution operation. It is

clear how F_{land} moves from 0 (black) to 1 (red) as the measurements cross from open ocean to land.

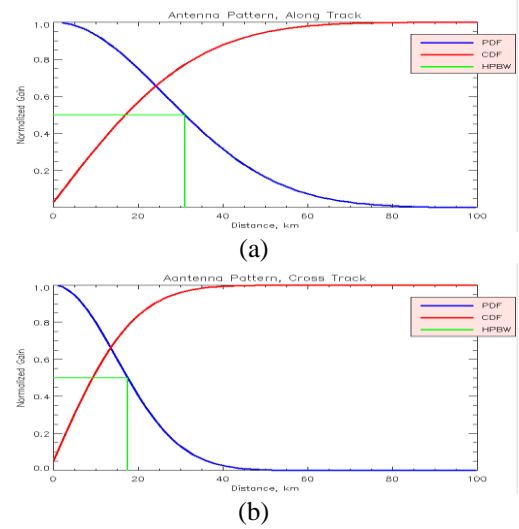


Figure 2: Gaussian function used to simulate the AMSR2 6GHz channel antenna. Panels a and b show the along- and cross-track patterns, respectively.

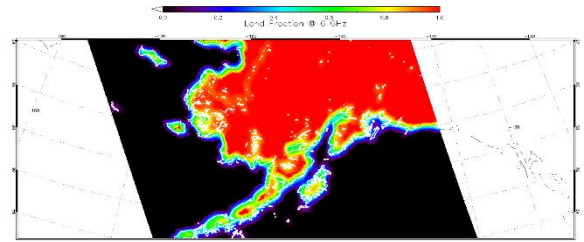


Figure 3: Calculated land fraction for AMSR2 6 GHz channel around the coast of Alaska.

Lastly, we solve equation 1 for Tb_{water} where Tb_{meas} is the reported Tb in AMSR2 Level-1B (L1B) data, and Tb_{land} is a measured Tb, within the corresponding IFOV, with F_{land} equals to 1. A major challenge in this approach is to determine Tb_{land} which varies significantly with different land types. To overcome this issue, we used the higher frequency channels, particularly the 36 GHz H- and V-pol channels. The 89 GHz channels were excluded due to their high sensitivity to atmospheric parameters more than surface parameters.

The relatively small IFOV size of AMSR2 36 GHz channel allows Tb measurements very close to the coastline with minimal land contamination. Thus, the ratio of measured Tbs of the channel to be corrected and the 36 GHz channel was used as a boundary condition on the corrected Tbs.

Figure 4 shows AMSR2 Tbs before (panels a, b, and c) and after applying the correction (panels d, e, and f) for the 6GHz, 7 GHz, and 10 GHz H-pol channels. Color indicates Tb values from 75–100 K, suitable for open ocean Tbs. The color bar saturates at 100 K to demonstrate the effect of land on measured Tbs before and after correction.

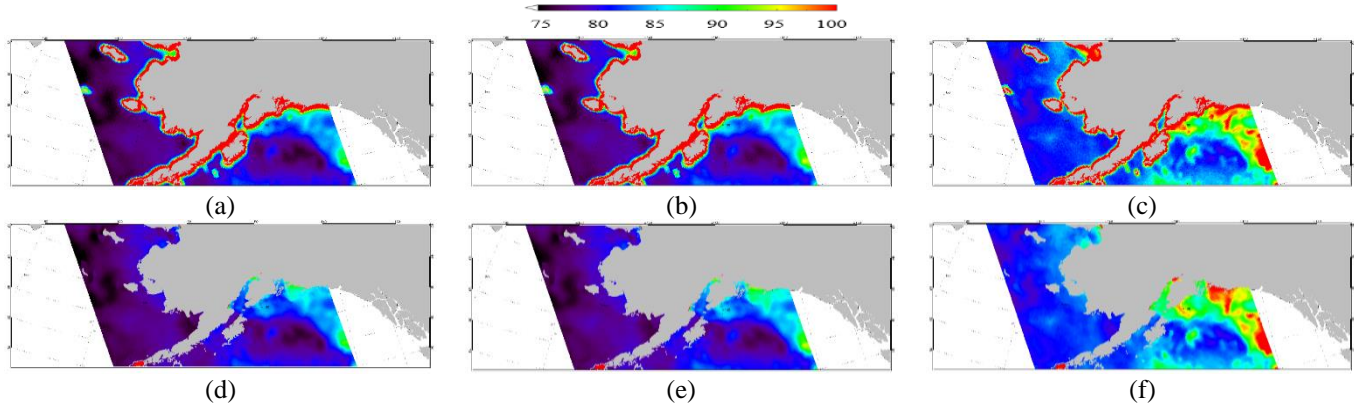


Figure 4: AMSR2 Tbs at 6 GHz (a and d), 7 GHz (b and e) and 10 GHz (c and d). The top and bottom rows represent AMSR2 Tbs before and after correction, respectively. Color indicates Tb values from 75 (black) to 100 (red) K.

Note that the corrected Tbs blend seamlessly with the surrounding open ocean measurements and the variations can be attributed to surface and atmospheric parameters.

4. CONCLUSIONS

In this paper we briefly described the methodology and the results of correcting AMSR2 for land contamination. Corrected Tbs play a significant role in extending the usability of AMSR2 measurements to coastal areas and inland bodies of water. This will lead to having critical geophysical parameters retrieved closer to land, which is important for fishing activities, protecting marine life, and protecting lives and property in the case of extreme wind events. AMSR2 was selected as an application example, but the concept can be applied more generally to other microwave radiometers with large IFOVs.

Results from the described technique are promising but requires more validation. The validation plan is to use the corrected Tbs to retrieve geophysical parameters and then compare retrievals with numerical weather models and in situ measurements. It is worth noting that this is a work in progress and a follow-on paper is in preparation to describe in full details the development, implementation, and validation of AMSR2 coastal correction and coastal products.

5. ACKNOWLEDGEMENT

The scientific results and conclusions, as well as any views or opinions expressed herein, are those of the author(s) and do not necessarily reflect those of NOAA or the Department of Commerce.

6. REFERENCES

[1] F. T. Ulaby and D. G. Long, "Microwave Radar and Radiometric Remote Sensing," University of Michigan Press, pp. 1016, 2014

[2] N. C. Grody, "Remote sensing of atmospheric water content from satellites using microwave radiometry," *IEEE Trans. Antennas Propag.*, vol. 24, no. 2, pp. 155–162, Mar. 1976.

[3] T. T. Wilhelm and A. T. C. Chang, "An algorithm for retrieval of ocean surface and atmospheric parameters from the observations of the scanning multichannel microwave radiometer," *Radio Sci.*, vol. 15, pp. 525–544, 1980.

[4] S. O. Alswiss, Z. Jelenak, and P. S. Chang, "Remote Sensing of Sea Surface Temperature Using AMSR2 Measurements," *IEEE J. Sel. Topics Appl. Earth Observ. Remote Sens.*, vol. 10, no. 10, pp. 3948–3954, 2017.

[5] P. C. Meyers and R. R. Ferraro, "Precipitation from the Advanced Microwave Scanning Radiometer 2," in *IEEE Journal of Selected Topics in Applied Earth Observations and Remote Sensing*, vol. 9, no. 6, pp. 2611–2618, June 2016.

[6] S. O. Alswiss, P. Laupattarakasem and W. L. Jones, "A Novel Ku-Band Radiometer/Scatterometer Approach for Improved Oceanic Wind Vector Measurements," in *IEEE Transaction on Geosciences and Remote Sensing*, vol. 49, no. 9, pp. 3189–3197, Sept. 2011.

[7] S. O. Alswiss, Z. Jelenak, P. S. Chang, J. D. Park, and P. Meyers, "Intercalibration results of the advanced microwave scanning radiometer-2 over ocean," *IEEE J. Sel. Topics Appl. Earth Observ. Remote Sens.*, vol. 8, no. 9, pp. 4230–4238, 2015.

[8] NOAA's GCOM-W program products webpage: <https://manati.star.nesdis.noaa.gov/gcom/datasets/GCOM2Data.php>

[9] J. X. Yang, D. S. Mckague, and Ruf, C. S. (2014). Land Contamination Correction for Passive Microwave Radiometer Data: Demonstration of Wind Retrieval in the Great Lakes Using SSM/I, *Journal of Atmospheric and Oceanic Technology*, 31(10), 2094–2113

[10] P. Wessel, W. H. F. Smith, R. Scharroo, J. Luis, and F. Wobbe, "Generic Mapping Tools: Improved Version Released," *Eos Trans. AGU*, vol. 94, no. 45, pp. 409–410, 2013.